Aqueous Method Synthesis and Characterization of SiO2@CsPbBr3 Thin Film Structured Materials

Yogesh Ghogare[1], Mamata R. Lanjewar[2], Arjun Mane[1], Sanjay R. Thakare[1*] and Twinkle S. Wankhede[3]

[1]*Government Institute of Forensic Science, Civil Lines, India.*
[2]*Department of Chemistry, P.G.T.D. Rashtrasant Tukadoji Maharaj Nagpur University, India.*
[3]*Department of Chemistry, Dr. Ambedkar College, Deekshabhoomi, India*
Email: sanjaythakareisc@gmail.com

Abstract: Nanocrystalline CsPbBr3 and CsPbBr3 phosphor layers were successfully deposited onto monodisperse, spherical, and non-aggregated SiO2 particles using an aqueous synthesis method. This process led to the formation of SiO2@CsPbBr3 thin-film structured materials. The structural, morphological, and optical properties of the resulting materials were systematically investigated through X-ray diffraction (XRD), scanning electron microscopy (SEM), photoluminescence (PL) spectroscopy, and UV-visible absorption spectroscopy. XRD results confirmed the successful coating of CsPbBr3 layers on the SiO_2 surfaces, this finding further verified by SEM images. The photoluminescence spectra revealed that the SiO2@CsPbBr3 thin film materials exhibited a prominent green emission band, with maximum at 507 nm, indicating their potential in optoelectronic and photonic applications.

Keywords: Aqueous synthesis, SiO_2@$CsPbBr_3$, nanocrystalline, photoluminescence, thin-film materials.

1. Introduction

A chemical compounds which are structurally similar to the mineral perovskite $CaTiO_3$ are numerous and this class of compounds is known as perovskite. The ideal structure of perovskite is ABX_3 having a BX_6 corner-sharing octahedra while 12-fold coordination A cation formed a cube of eight such octahedrons formed perfect structure. This class of crystalline structures was paid more attention recently because of a large number of elements that can occupy the A, B and X sites, which result in a very wide variety of physical properties. Notwithstanding the fact that perovskite class of compounds have been well known for number of decades [1], the recent progress in the synthesis of lead-based hybrid organic–inorganic perovskites and their application in the variety of optoelectronics devices [2] has been attracted scientific community largely. An organic cation in A site, an inorganic cation (commonly Pb^{2+}) in B site and a halide in X site makes hybrid perovskite, which is innovative materials for many applications [3–5], especially related to solar energy conversion and the fabrication of diodes, lasers, light-emitting diodes (LEDs), and many others [5-7]. Their good capability of adsorbing light, long diffusion length of charge carriers, and tunable band gap, are their main advantages with respect to traditional materials. In spite of their high efficiency, there are some drawbacks, the most important of which is the lack of chemical and structural stability [8-10].

An exposure of moisture [11], ultraviolet (UV) irradiation [9,10,12] or heat [13,14] to the organic lead halide perovskites shows rapid degradation. The rapid degradation of organic lead halide perovskites was observed because of instability of organic cations which undergoes hydration reaction [15,16]. A completely inorganic lead halide perovskites have been synthetized by changing organic cations with inorganic ones is a way to solve this issue [17]. All inorganic lead halide perovskites having larger stability which is important for practical applications [18] but having slightly inferior optical properties compared to organic lead halide perovskites. $CsPbBr_3$ is one of the most studied and promising completely inorganic perovskites because of its easy synthesis and gainful direct bandgap (2.3 V) [19].

Two different approaches were proposed for the synthesis of thin film of $CsPbBr_3$ and other perovskite materials via wet chemistry deposition. In one, stoichiometric amount of precursor salts is mixed together in a one solvent and mixed solution was applied on the surface of substrate followed by evaporation of solvent to leaving behind the perovskite deposition. While in alternative approach, the precursors salts are dissolved in two different solvents and independently deposited on the substrate by different methods such as spin coating, deep coating or spray coating followed by thermal treatment to form the perovskite [7,20]. Inappropriately, these processes generally produce incoherent films composed of tiny separated single crystals. As a result, large grain boundaries are produced which increases the recombination rate subsequently system efficiency decreases. Deposition via melting of both precursor salts in a quartz tube has also been proposed but this approach turned out to be not appropriate for industrial applications [21]. Recently, new, easy, and fast process was proposed for the deposition of thin, uniform, and chemically homogeneous perovskite films using magnetron sputtering technology [22].
The intention of this work was to organized CsPbBr3 deposited onto silica gel coted thin film substrates in presence of atmospheric conditions without using any sophisticated aids. This technique will be adequate to prepare the perovskite films on any substrates such as soda lime glass, quartz glass, polycrystalline gold, indium tin oxide (ITO) which is generally used for future application in field of optoelectronic devices.

2. Materials and Methods

All the chemicals and reagents used in this study were purchase from Merck and used as received without any further purification. A 1 mM solution of cesium bromide was prepared by dissolving the appropriate amount of the salt in double distilled water under continuous magnetic stirring for 10 minutes to ensure complete dissolution. Subsequently, a 1 mM solution of lead bromide in double distilled water was added dropwise to the cesium bromide solution while maintaining constant stirring at a temperature of 50°C. Following the complete addition of the lead bromide solution, the resulting mixture was continuously stirred for an additional 60 minutes. The prepared solution was then left undisturbed at room temperature for 24 hours to allow for proper aging and stabilization. After this period, the mixture was stirred again for 30 minutes to homogenize the contents. The final solution was applied on the pre-cleaned silica plates using a spray-coating technique. The coated silica plates were then dried gradually in a hot air oven under controlled conditions. Once fully dried, the prepared silica plates were stored in a dry, dust-free environment until further use in subsequent experiments.
X-ray diffraction patterns were recorded X-ray diffractometer (XRD-Shimadzu 500) using Cu-Kα radiation from an X-ray source, operating at 40 kV and 30 mA. The samples were characterized by scanning electron microscopy (ZEISS Gemini SEM microscope 500) to acquire pictures for scanning electron microscopy (SEM) images The UV-visible absorption spectra were recorded with an UV-Vis spectrophotometer (LabIndia analytical UV-3000, LabIndia, Navi Mumbai, India). Photoluminescence (PL) spectra were taken on a Shimadzu RF-5301 PC spectroflurophotometer, and a 450W Xe-lamp was used as the excitation source.

3. Result and Discussion

The XRD patterns of silica gel thin film, $CsPbBr_3$ and SiO_2@$CsPbBr_3$ molecule are shown in Fig. 1. It is observed that the silica gel thin film which is generally used for thin film chromatography having characteristics peak of amorphous SiO_2 (JCPDS No. 29-0085) at broad band centered at $2\theta = 22.00^{\circ}$. No other diffraction peak corresponding to SiO_2 is observed except this. In case of SiO_2@$CsPbBr_3$ material obtained shows broad band at $2\theta = 22.00^{\circ}$ from amorphous SiO_2, all the diffraction peaks belonging to crystalline $CsPbBr_3$ are present, suggesting that the coatings of $CsPbBr_3$ have crystallized well on the surfaces of amorphous silica particles. No other phase has been detected, indicating that no reaction occurred between the SiO_2 support particles and thin film of $CsPbBr_3$ particle coted on. In general, the nanocrystalline size can be estimated from the Scherrer formula using x-ray wavelength 0.154 nm [23]. Here we take diffraction data in the (100), (110), (200), (201), (211) and (202) planes to calculate the nanocrystalline sizes of $CsPbBr_3$ particle on the surface of SiO_2, and the estimated average crystallite size is 36 nm.

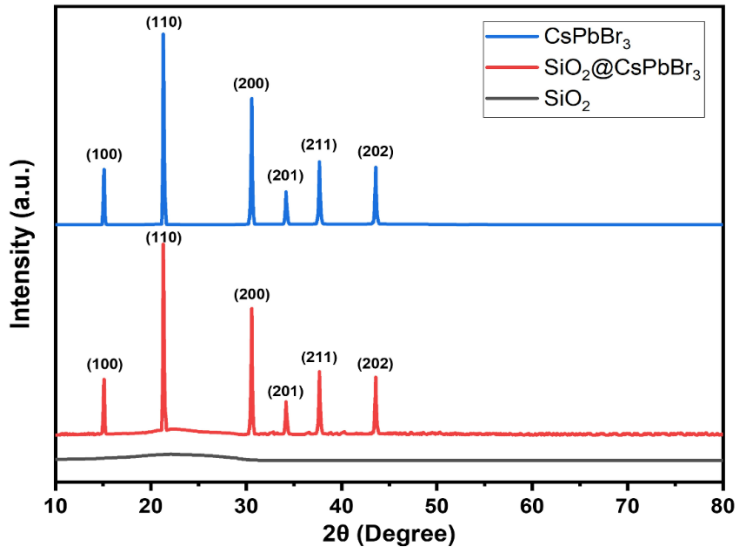

Figure 1. XRD patterns of silica gel thin film, SiO_2@$CsPbBr_3$ and $CsPbBr_3$ prepared by aqueous method.

To investigate the morphological characteristics of the synthesized samples, scanning electron microscopy (SEM) images of the "as-prepared" SiO_2@$CsPbBr_3$ material were obtained, as shown in Fig. 2. Despite the deposition process being conducted in an aqueous environment under consistent experimental conditions, the resulting films exhibited distinct and recognizable morphological features. Specifically, on the silica gel thin film, the deposited $CsPbBr_3$ formed uniformly distributed nanoscale grains covering the entire surface. This uniform distribution of nanocrystalline grains is indicative of the effective and homogeneous coating achieved by the aqueous deposition method.

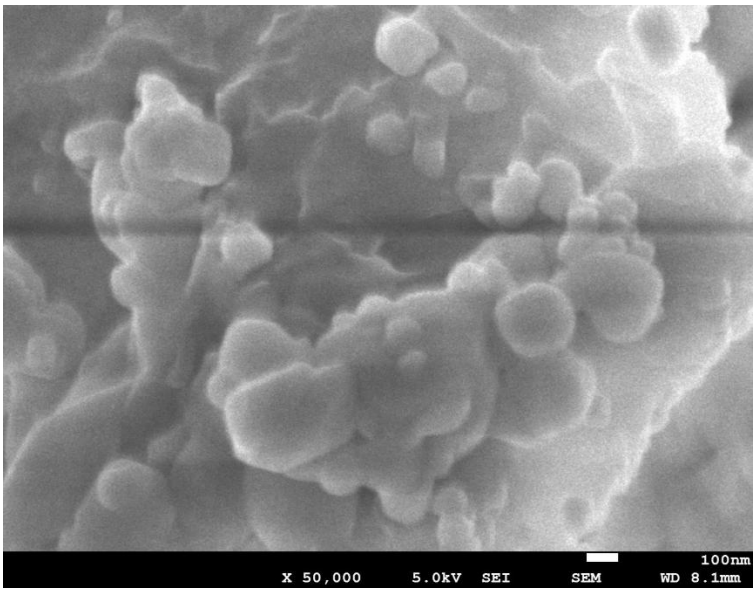

Figure 2. SEM images of the "as-prepared" samples of SiO_2@$CsPbBr_3$

The optical properties of the synthesized SiO_2@$CsPbBr_3$ films were evaluated by measuring their light absorption behavior using UV–Visible absorption spectroscopy. These measurements provide valuable insight into the optical response and bandgap characteristics of the material. As illustrated in Fig. 3, the UV–Visible absorption spectrum of the SiO_2@$CsPbBr_3$ composite is presented as a function of wavelength. The observed absorption features reflect the presence of the $CsPbBr_3$ nanocrystalline layer and its interaction with incident light, confirming the successful formation of the perovskite thin film on the SiO_2 substrate.

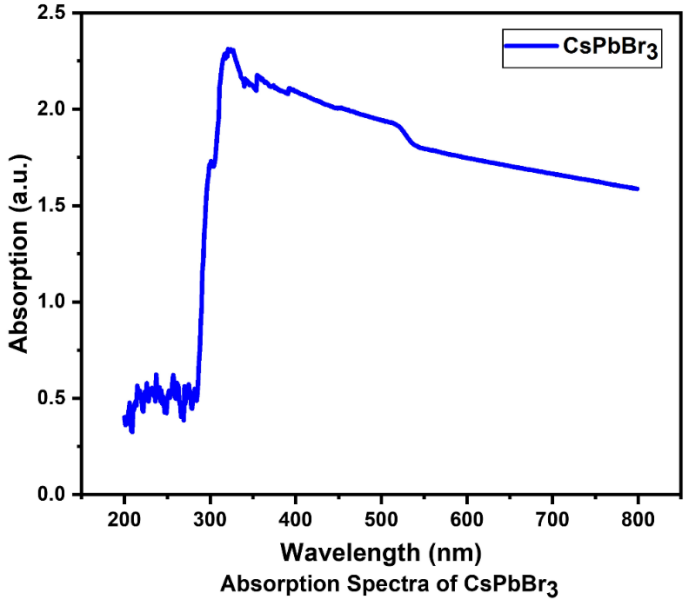

Figure 3. UV–Visible absorption spectra SiO_2@$CsPbBr_3$ material

In UV–Visible absorption spectra, the absorption edge is typically used to estimate the optical bandgap of a material. In the case of the SiO_2@$CsPbBr_3$ material, absorption edge was observed, corresponding to the characteristic electronic transition of the $CsPbBr_3$ perovskite layer. Based on this absorption edge, the optical bandgap of the SiO_2@$CsPbBr_3$ material was determined to be approximately 2.75 eV.
The photoluminescence properties of the SiO_2@$CsPbBr_3$ thin-film materials were examined by using a spectroflurophotometer to monitor the emitted light as a function of wavelength. This technique provides important information about the optical emission behavior and electronic transitions within the material. As shown in Fig. 4, the emission spectrum of the SiO_2@$CsPbBr_3$ material displays a distinct photoluminescence peak, confirming the characteristic light-emitting properties of the $CsPbBr_3$ nanocrystalline layer. The spectral profile and emission intensity further verify the successful formation of the luminescent perovskite coating on the SiO_2 particles.

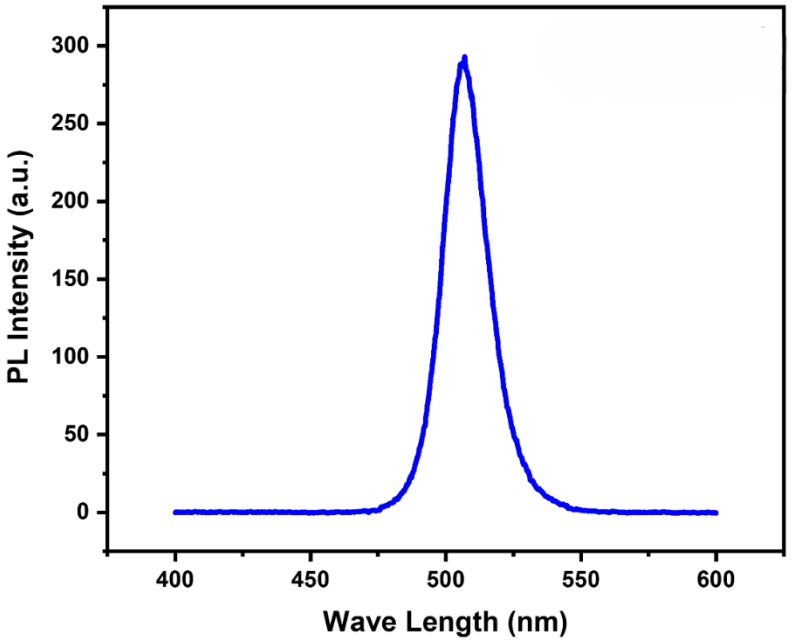

Figure 4. Emission spectra SiO_2@$CsPbBr_3$ material

As illustrated in Fig. 4, the SiO_2@$CsPbBr_3$ thin-film material exhibits a strong photoluminescence emission peak centered at 507 nm, corresponding to a bright green light emission. This prominent

emission indicates the effective incorporation of the $CsPbBr_3$ perovskite layer on the SiO_2 and reflects the material's excellent light-emitting capability. The relatively high emission intensity further highlights the optical quality and luminescent efficiency of the synthesized material, making it a promising candidate for applications in light-emitting and optoelectronic devices [24].

4. Conclusions

In this study, a simple, cost-effective, and environmentally friendly aqueous synthesis method successfully developed for the uniform coating of $CsPbBr_3$ layers onto monodisperse, spherical SiO_2 particles. The resulting SiO_2@$CsPbBr_3$ thin-film material exhibited spherical morphology, uniform particle size, and a narrow size distribution, demonstrating the excellent structural integrity. Under UV excitation, these materials exhibit intense and stable green photoluminescence, confirming both the successful deposition and optical functionality of the $CsPbBr_3$ coating. The excellent structural and optical properties of the SiO_2@$CsPbBr_3$ thin-film materials highlight their promising potential for use in optoelectronic devices, photonic technologies, and light-emitting applications.

Funding Details
The authors did not receive any financial support for this research

References

1. Rao, C. N. R. (2001). Perovskites. In R. A. Meyers (Ed.), Encyclopedia of Physical Science and Technology (3rd ed., pp. 707–714). Academic Press.
2. Green, M. A., & Ho-Baillie, A. (2017). Perovskite solar cells: The birth of a new era in photovoltaics. ACS Energy Letters, 2(4), 822–830.
3. Huang, J., Yuan, Y., & Thompson, B. C. (2018). World Scientific Handbook of Organic Optoelectronic Devices: Volume 1: Perovskite Electronics. World Scientific Publishing.
4. Stranks, S. D., & Snaith, H. J. (2015). Metal-halide perovskites for photovoltaic and light-emitting devices. Nature Nanotechnology, 10(5), 391–402.
5. Wu, J. R., Thakur, D., Chiang, S. E., Chandel, A., Wang, J. S., Chiu, K. C., & Chang, S. H. (2019). The way to pursue truly high-performance perovskite solar cells. Nanomaterials, 9(9), 1269.
6. Kanemitsu, Y., & Handa, T. (2018). Photophysics of metal halide perovskites: From materials to devices. Japanese Journal of Applied Physics, 57(9), 090101.
7. Chen, Y., Zhang, L., Zhang, Y., Gao, H., & Yan, H. (2018). Large-area perovskite solar cells–A review of recent progress and issues. RSC Advances, 8(19), 10489–10508.
8. Wang, D., Wright, M., Elumalai, N. K., & Uddin, A. (2016). Stability of perovskite solar cells. Solar Energy Materials and Solar Cells, 147, 255–275.
9. Shirayama, M., Kato, M., Miyadera, T., Sugita, T., Fujiseki, T., Hara, S., Kadowaki, H., Murata, D., Chikamatsu, M., & Fujiwara, H. (2016). Optical transitions in hybrid perovskite solar cells: Ellipsometry, density functional theory, and quantum efficiency analyses for $CH_3NH_3PbI_3$. Physical Review Applied, 5(1), 014012.
10. Wang, F., Ma, J., Xie, F., Li, L., Chen, J., Fan, J., & Zhao, N. (2016). Organic cation-dependent degradation mechanism of organotin halide perovskites. Advanced Functional Materials, 26(21), 3417–3423.
11. Calisi, N., Caporali, S., Milanesi, A., Innocenti, M., Salvietti, E., & Bardi, U. (2018). Composition-dependent degradation of hybrid and inorganic lead perovskites in ambient conditions. Topics in Catalysis, 61(13–14), 1201–1208.
12. Lanzetta, L., Aristidou, N., & Haque, S. A. (2020). Stability of lead and tin halide perovskites: The link between defects and degradation. The Journal of Physical Chemistry Letters, 11(2), 574–585.
13. Akbulatov, A. F., Frolova, L. A., Dremova, N. N., Zhidkov, I., Martynenko, V. M., Tsarev, S. A., Luchkin, S. Y., Kurmaev, E. Z., Aldoshin, S. M., & Stevenson, K. J. (2020). Light or heat: What is killing lead halide perovskites under solar cell operation conditions? The Journal of Physical Chemistry Letters, 11(2), 333–339.
14. Ava, T. T., Mamun, A. A., Marsillac, S., & Namkoong, G. (2019). A review: Thermal stability of methylammonium lead halide based perovskite solar cells. Applied Sciences, 9(2), 188.
15. Zhang, C. X., Shen, T., Guo, D., Tang, L. M., Yang, K., & Deng, H. X. (2020). Reviewing and understanding the stability mechanism of halide perovskite solar cells. InfoMat, 2(5), 1034–1056.
16. Kim, B., & Seok, S. I. (2020). Molecular aspects of organic cations affecting the humidity stability of perovskites. Energy & Environmental Science, 13(3), 805–820.
17. Li, Z., Song, C., Rao, L., Lu, H., Yan, C., Cao, K., Ding, X., Yu, B., & Tang, Y. (2019). Synthesis of highly photoluminescent all-inorganic $CsPbX_3$ nanocrystals via interfacial anion exchange reactions. Nanomaterials, 9(9), 1296.

18. Kulbak, M., Gupta, S., Kedem, N., Levine, I., Bendikov, T., Hodes, G., & Cahen, D. (2016). Cesium enhances long-term stability of lead bromide perovskite-based solar cells. The Journal of Physical Chemistry Letters, 7(1), 167–172.
19. Kulbak, M., Cahen, D., & Hodes, G. (2015). How important is the organic part of lead halide perovskite photovoltaic cells? Efficient $CsPbBr_3$ cells. The Journal of Physical Chemistry Letters, 6(13), 2452–2456.
20. Zhang, J., Hodes, G., Jin, Z., & Liu, S. F. (2019). All-inorganic $CsPbX_3$ perovskite solar cells: Progress and prospects. Angewandte Chemie International Edition, 58(44), 15596–15618.
21. Stoumpos, C. C., Malliakas, C. D., Peters, J. A., Liu, Z., Sebastian, M., Im, J., Chasapis, T. C., Wibowo, A. C., Young Chung, D., Freeman, A. J., & Kanatzidis, M. G. (2013). Crystal growth of the perovskite semiconductor $CsPbBr_3$: A new material for high-energy radiation detection. Crystal Growth & Design, 13(7), 2722–2727.
22. Borri, C., Calisi, N., Galvanetto, E., Falsini, N., Biccari, F., Vinattieri, A., Cucinotta, G., & Caporali, S. (2020). First proof-of-principle of inorganic lead halide perovskites deposition by magnetron-sputtering. Nanomaterials, 10(1), 60.
23. Birks, L. S., & Friedman, H. (1946). X-ray spectrochemical analysis. Journal of Applied Physics, 17(11), 687–692.
24. Protesescu, L., Yakunin, S., Bodnarchuk, M. I., Krieg, F., Caputo, R., Hendon, C. H., Yang, R. X., Walsh, A., & Kovalenko, M. V. (2015). Nanocrystals of cesium lead halide perovskites ($CsPbX_3$, X = Cl, Br, and I): Novel optoelectronic materials showing bright emission with wide color gamut. Nano Letters, 15(6), 3692–3696.